LETTERS

Orbital forcing of Cretaceous river discharge in tropical Africa and ocean response

Britta Beckmann[1], Sascha Flögel[2], Peter Hofmann[3], Michael Schulz[1,4] & Thomas Wagner[5]

The tropics have been suggested as the drivers of global ocean and atmosphere circulation and biogeochemical cycling during the extreme warmth of the Cretaceous period[1,2]; but the links between orbital forcing, freshwater runoff and the biogeochemistry of continental margins in extreme greenhouse conditions are not fully understood. Here we present Cretaceous records of geochemical tracers for freshwater runoff obtained from a sediment core off the Ivory Coast that indicate that alternating periods of arid and humid African climate were driven by orbital precession. Our simulations of the precession-driven patterns of river discharge with a global climate model suggest that ocean anoxia and black shale sedimentation were directly caused by high river discharge, and occurred specifically when the northern equinox coincided with perihelion (the minimum distance between the Sun and the Earth). We conclude that, in a warm climate, the oceans off tropical continental margins respond rapidly and sensitively to even modest changes in river discharge.

Intervals of extreme warmth and enhanced sequestration of marine organic carbon (OC), termed oceanic anoxic events (OAEs), are one focus of current palaeoclimate research. They provide fundamental information on the functioning of biogeochemical cycles and their feedbacks during extreme conditions, especially when applied to areas expected to react sensitively to climate change, that is, continental margins and their associated sub-basins. Deposits from the eastern tropical Atlantic Ocean at ODP Site 959 off the Ivory Coast were obtained from such a setting (Fig. 1), providing a unique record of Coniacian to Campanian OC-rich sedimentation that covers the last of the Cretaceous OAEs (OAE 3). OAE 3 black shales have been reported from various basins surrounding the Atlantic and Tethyan Margin[3–5]. Millennial-scale OAE 3 records from ODP Site 959 were used to develop a model for black shale formation in the tropical Atlantic[6]. Additionally, records of quartz and clay mineralogy document Upper Cretaceous atmospheric circulation that triggered latitudinal shifts of African climate belts. The records further imply that black shales formed in response to tropical continental discharge that induced stratification and reversals in surface ocean circulation within the deep Ivorian basin (DIB)[6]. Synchronous variations in trace metals[7] and biomarkers of green sulphur bacteria[8] further provide evidence for severe variations in redox conditions, with brief intervals of lower photic zone euxinia[8]. Here we present records that double the stratigraphic range of the previous profiles into the lower Campanian, allowing the deduction of long-term trends and shorter-scale variations in the tropical atmosphere–ocean system across one of the most important transitions in global climate over the past 150 Myr.

Coniacian–Campanian African climate variability is evident from fluctuations of K/Al and Ti/Al ratios (Fig. 2a, b). Al is mainly confined to the fine-grained aluminosilicate fraction[9], typically enriched in kaolinite, smectite and iron hydroxides[10], and formed by intense chemical weathering under warm and humid conditions. K is associated with continental siliciclastics (that is, clay minerals and feldspar) that experienced only moderate amounts of chemical alteration[11]. Ti is concentrated in heavy minerals and often transported via aeolian pathways into marine sediments[12]. In agreement with vegetation simulations for the Campanian[13], the source for Ti is assigned to desert areas of the proto-Kalahari in southern Africa, while K is associated with illite and K-feldspar derived from semi-arid tropical regions. Al from kaolinite and smectite is indicative of tropical weathering in equatorial northern Africa[6,10,12]. The persistent periodicity of climate tracers at Site 959 documents that Upper Cretaceous climate was highly variable and modulated at different timescales. The average K/Al record exhibits a long-range increase towards the top of the profile (Fig. 2b). The progression in supply of detrital material from semi-arid regions supports a gradual aridification of Africa that started in the lower Santonian. The linearity of the complementary Ti/Al record indicates the existence of an arid proto-Kalahari remaining constant in extension and geographical position.

Time–frequency analyses of the K/Al and Ti/Al records support the existence of one dominant period with ~1.3 m wavelength, equivalent to ~28 kyr in nannofossil biozone CC15. Given uncertainties in

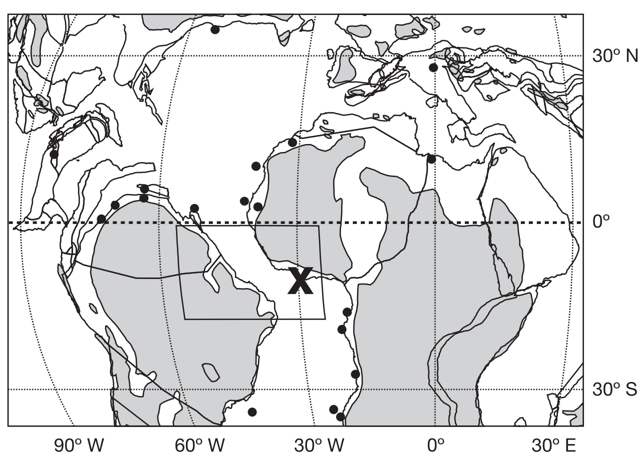

Figure 1 | Location of OAE 3 sites and investigated region for simulated river discharge. ODP Site 959 is marked by X; dots indicate other reported OAE 3 sites[8]; black box marks investigated region for simulated river discharge. All information is superimposed on the palaeogeographic map of the Upper Cretaceous ~80 Myr ago[20]. Grey shaded areas represent land masses.

[1]Department of Geosciences, University of Bremen, Klagenfurter Str., 28357 Bremen, Germany. [2]IFM – GEOMAR Leibniz Institute of Marine Sciences, FB 1, Ocean Circulation and Climate Dynamics, Wischhofstr. 1-3, 24148 Kiel, Germany. [3]Institute for Geology and Mineralogy, University of Cologne, Zülpicher Str. 49a, 50674 Köln, Germany. [4]Research Center Ocean Margins, University of Bremen, Leobener Str., 28357 Bremen, Germany. [5]School of Civil Engineering and Geosciences, University of Newcastle, Newcastle upon Tyne NE1 7RU, UK.

Table 1 | Simulated river discharge

Orbital case	Perihelion at	Northern Hemisphere	Seasonal contrasts	Total annual discharge ($km^3 yr^{-1}$)*	Wet season relative to annual discharge (%)	Wet season discharge, Mar.–Jun. ($km^3 yr^{-1}$)	Dry season discharge, Jul.–Feb. ($km^3 yr^{-1}$)	Thickness of annual freshwater lid (m)
Orb. A	Northern spring equinox	Warm spring/ cold autumn	Max.	1,556 (+43%)	71	1,101 (+79%)	288 (−27%)	1.00
Orb. B	Northern winter solstice	Trans.	Trans.	1,365 (+25%)	67	917 (+49%)	276 (−30%)	0.88
Orb. C	Northern autumn equinox	Cold spring/warm autumn	Min.	1,091 (0%)	56	614 (0%)	393 (0%)	0.70
Orb. D	Northern summer solstice	Trans.	Trans.	1,343 (+23%)	63	851 (+39%)	407 (+4%)	0.86

Simulated continental freshwater discharge for the investigated region. The analysed area was situated in tropical, Upper Cretaceous Africa and South America (3,945,198.69 km^2); the resulting thickness of the freshwater lid in the Equatorial Atlantic for all simulations is expressed as total values in $km^3 yr^{-1}$, relative proportions, and metres. Max., maximum; trans., transitional; min., minimum.
*Relative to Orb. C.

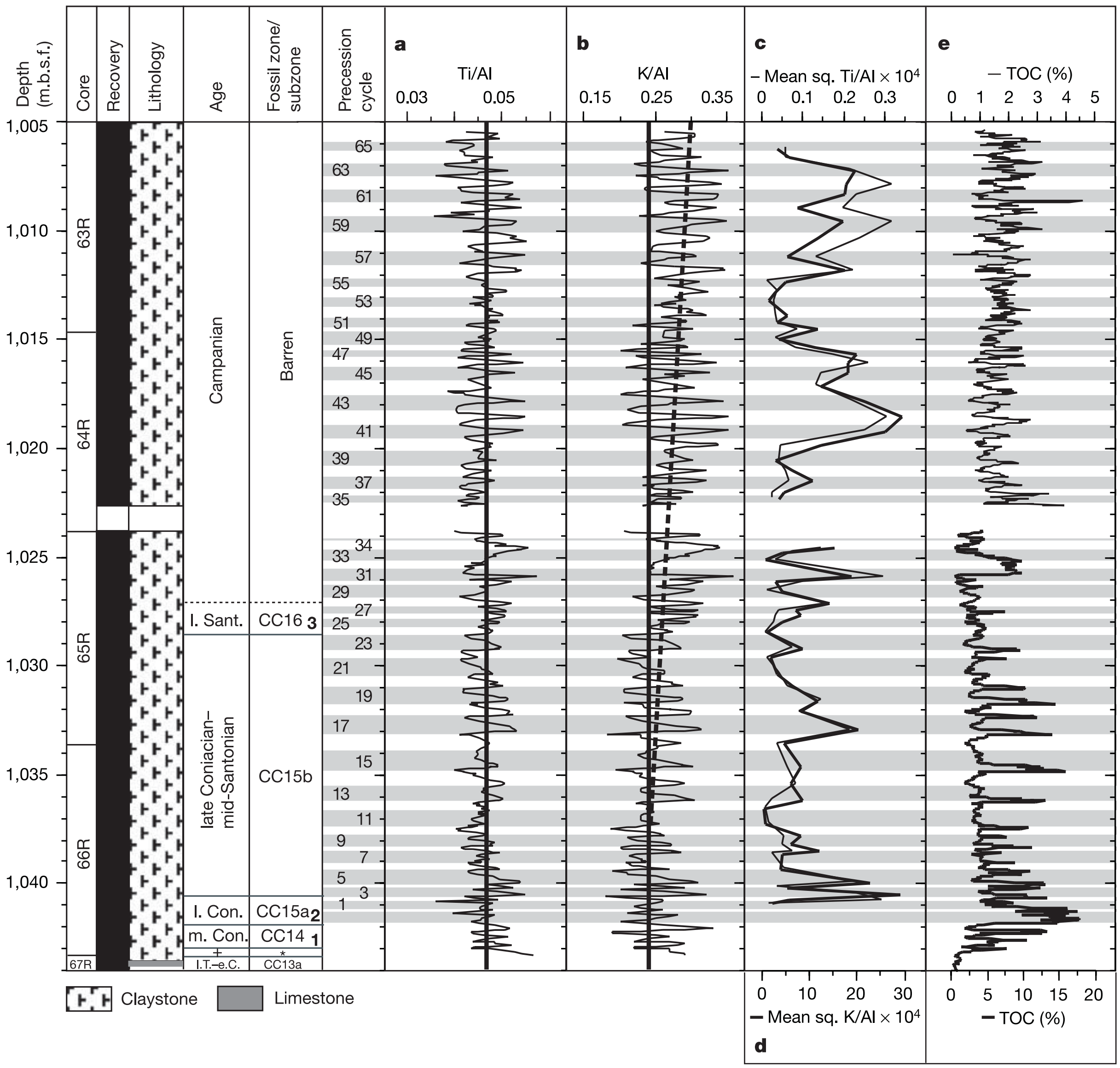

Figure 2 | Upper Cretaceous (Coniacian to Campanian) records from ODP Site 959. **a**, Ti/Al ratio, average value indicated by solid black line. **b**, K/Al ratio, average value for lower part of the profile indicated by solid line, mean values starting from 1,034 m.b.s.f., marked by dashed line. Both proxies (**a**, **b**) serve as a measure of fluctuations between tropical and arid climate conditions; higher values indicate greater aridity. **c**, Mean square Ti/Al values (thin line). **d**, Mean square K/Al values (heavy line). Both proxies (**c**, **d**) are calculated as the standard deviation from respective mean values for each precession cycle; higher values indicate greater seasonality, that is, more marked alternations between arid and humid conditions. **e**, Total organic carbon content (TOC) in %; bottom axis refers to values below 1,022.5 m.b.s.f. (heavy line); top axis refers to data above 1,022.5 m.b.s.f. (thin line). Higher values (15–20%) indicate anoxia. Fossil zone/subzone and age from refs 21, 22; l. Sant., late Santonian; l. Con., late Coniacian; m. Con., mid Coniacian; l. T.–e. C., late Turonian to early Coniacian; *CC13b; + early Coniacian; absolute ages[23]; 1, 87.2 Myr; 2, 85.5 Myr; 3, 84.8 Myr. Precession cycles (numbered from bottom to top) below 1,024 m.b.s.f. are based on previous work[6,8].

time control and sedimentation rate at Site 959, we conclude that this prominent periodicity lies close enough to 22 kyr to support the influence of precession. (Details of the time–frequency analysis are available as Supplementary Information.) Given the persistence of the dominant periodicity with respect to total organic carbon (TOC) burial across the core break above 1,022.5 metres below the sea floor (m.b.s.f.), we estimate 65 cycles for the entire section (1,044–1,005 m.b.s.f.), equivalent to ~1.46 Myr. Variance records of K/Al and Ti/Al reveal the evolution of African climate contrasts (Fig. 2c, d). High values document alternations between arid and humid conditions, and low values indicate more balanced climate. Above 1,022.5 m.b.s.f. a robust pattern consisting of 19 cycles emerges (Fig. 2c, d), corresponding to the ~400 kyr period. The variance records below 1,022.5 m.b.s.f. show a frequency with a periodicity of ~315 kyr (~14 cycles in total). This regularity is not attributable to the main orbital frequencies, and cannot easily be explained. We consider the manifestation of a 400 kyr periodicity to be the expression of a long-term drying/cooling cycle. The presence of long eccentricity and precession cycles supports Upper Cretaceous climate as having been dynamic and variable, comparable to that of the Quaternary.

A linkage of African continental climate with OC burial and oceanic productivity on a precession cycle level has been reported before[6–8], and is evident when the Coniacian–Campanian OC record from Site 959 is compared to the Ti/Al and K/Al profiles. The section below 1,024 m.b.s.f. displays a distinct cyclic, high-amplitude pattern[8] that fades out towards the top owing to the progressive subsidence of Site 959 through time[14,15] (Fig. 2e). Despite the decline in amplitudes, maxima in OC generally coincide with minima in K/Al and Ti/Al, that is, with periods of enhanced detrital input from tropical source areas.

OC accumulation within individual cycles exhibits a distinct pattern (Fig. 2e) characterized by an initial sharp increase followed by a plateau and a gradual decrease. Only peak OC deposition was associated with the development sea floor anoxia and photic zone euxinia[8]. A compilation of OC data from Late Coniacian–Mid Santonian nannofossil zone CC15 reveals that maximum black shale sedimentation on average lasted for a quarter cycle, that is, ~5 kyr (ref. 7). The robustness of this pattern across the record points to an external control that caused episodic anoxic conditions in the tropical eastern Atlantic over more than one million years. A previous investigation[6] proposed that black shale formation was triggered by discharge of freshwater and nutrients to the semi-enclosed DIB, resulting in a circulation reversal and the development of ocean anoxia/euxinia[6,8]. Although less well constrained, a similar mechanism and long-term climate trend has been suggested for the South American Maracaibo basin during OAE 3 (ref. 16).

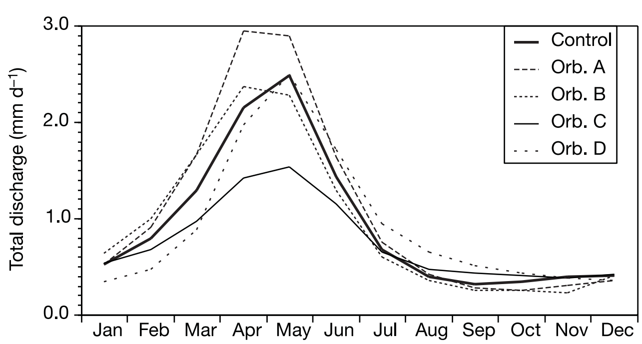

Figure 3 | Simulated total continental freshwater discharge over the course of one precession cycle (orbital cases A to D) compared to control run conditions. Total continental freshwater discharge (TD) was drastically enhanced during spring (April–May), independent of orbital configuration. Highest levels of up to 3 mm d^{-1} were achieved during orbital configuration A (warm spring/cold autumn in the Northern Hemisphere), in parallel with strongest seasonal contrasts. From orbital case A to C climate contrast diminishes, resulting in more balanced cold spring/warm autumn conditions and a decrease in TD by about a factor of 2 during orbital case C. Orbital cases B and D represent transitional phases.

The implications from the records of Site 959 were validated using global climate model GENESIS v.2.0 (ref. 17). (Details of the model and the experimental set-up of GENESIS v. 2.0 are available as Supplementary Information.) Five simulations with changing orbital configurations were conducted: a control run with no precession and four runs covering one precessional cycle, each shifting the closest annual approach of the Earth to the Sun (perihelion) into a different season.

Of specific relevance to the black shale mode is total freshwater discharge (TD). Previous simulations emphasized the importance of continental discharge for climate change and ocean response; for example, during the ice-free Early Eocene[18]. All simulations performed in this study yielded a pronounced wet season in spring and early summer (March to June, Fig. 3) with enhanced TD accounting for 56–71% of the total annual discharge (Table 1), and a dry season (July to February). Strongest seasonal contrasts occurred during orbital case A, representing the orbital configuration when spring is coincident with perihelion. Weakest contrasts are recognized for case C, suggesting most balanced conditions when perihelion coincided with autumn configuration. The two remaining orbital cases (B and D) describe 'transitional' modes. During case A, total annual TD was elevated by about 43% relative to case C. During the months of wettest conditions and largest divergence (March-June) TD was elevated by 79% (~487 km^3 yr^{-1}), but reduced by 27% (~105 km^3 yr^{-1}) during dry seasons (July–February) for case A relative to case C (Table 1).

The fluctuations in TD for orbital configurations A to D provide a robust mechanism to explain the observed pattern in ocean redox conditions and OC burial. Black shale formation apparently was restricted to case A, when maximum insolation (northern spring equinox at perihelion) occurred during wet seasons, both fostering seasonal contrasts and massive spring TD (Fig. 3). These conditions apparently were not reached during orbital configurations B, C and D. The runoff data suggest that a threshold in excess of 125 km^3 yr^{-1} was necessary to maintain a year-round or multi-year freshwater cap that triggered a reversal in ocean circulation in the DIB and a shift into a black shale mode. The estimated thickness of a freshwater cap ranges from 1.0 m during orbital case A to 0.7 m during orbital case C (Table 1), providing values comparable to the modern Black Sea (0.7 m; http://www.grid.unep.ch/bsein/index.html) but 2–3 times higher than for the modern Arctic Ocean (0.36 m)[19]. The direct linkage of African TD patterns and black shale formation in the DIB implies that fluctuations in ocean properties were short, that is, on seasonal timescales, but had a major effect on the Upper Cretaceous carbon cycle.

The results of this study demonstrate how sensitively and rapidly tropical marine areas close to continental margins react to even relatively moderate increases in continental freshwater discharge. The freshwater threshold required to shift sheltered and semi-enclosed areas of the modern ocean into an anoxic mode are unknown, but the progressive emission of greenhouse gases to the modern atmosphere is gradually shifting Earth towards a greenhouse mode with an accelerated hydrological cycle. At present it is hardly possible to estimate where we are on that long-term climate trend, but once the freshwater threshold is passed, a substantial impact on biochemical cycling of continental margins may be expected.

METHODS

Original data. Site 959 was drilled during ODP Leg159 off the Ivory Coast and Ghana at 3° 37.656′ N, 2° 44.149′ W in approximately 2,100 m water-depth. Samples were taken continuously in 1 cm increments, dried at 35 °C and homogenized before analysis. Determination of OC was performed after removal of inorganic carbon with 0.25 N HCl on every other sample. Major element chemistry was determined by X-ray fluorescence analysis on samples with an average spacing of every 8 cm.

Cycle and age model. The cyclostratigraphic model for the record of Hole 959D between 1,005.43 and 1,046.09 m.b.s.f. is based on the analysis of geochemical cycles within the interval below 1,022.5 m.b.s.f., in particular biozone CC15b[6]. In this biozone, the number of cycles in the Si/Al and K/Al records were matched to precession by counting the number of cycles in a biostratigraphically well-defined time interval. The cycle pattern with respect to the Si/Al, Ti/Al, K/Al and TOC records is not restricted to biozone CC15b, but clearly extends over the entire interval between 1,005.43 and 1,046.09 m.b.s.f. The biostratigraphic time control above 1,022.5 m.b.s.f., however, prohibits extending the approach described for biozone CC15b. Time–frequency analysis in CC15 reveals one prominent frequency of more than 3 cycles m^{-1} at the base that shifts to about 1.3 cycles m^{-1} above 1,037 m.b.s.f. The upper part of the profile between 1,022.69 and 1,005.43 m.b.s.f. also shows one prominent frequency at about 1.8 cycles m^{-1} that progressively decreases upward to about 1.3 cycles m^{-1}. No persistent signal components are detected at shorter wavelengths. The period of the dominant cycle in the time domain was estimated by analysing the data from nannofossil biozone CC15 above 1,041 m.b.s.f. in a chronostratigraphic framework. Time–frequency analysis for TOC and K/Al displays one prominent frequency at about 35 cycles Myr^{-1} throughout the main parts of the record. Based on the age model, this frequency corresponds to a period of about 28 kyr; this is close enough to 22 kyr to support precession as the prominent frequency. See Supplementary Information for further details.

Global circulation model. The general features of the GENESIS (Global Environmental Ecological Simulation of Interactive Systems) 2.0, designed for palaeoclimate research, have been presented before[13]. Boundary conditions were set for Cenomanian–Turonian simulations (see Supplementary Information for specifications of experimental set-up, palaeogeography, astronomical forcing, and validation of GENESIS v. 2.0). Five simulations with changing orbital forcing were carried out.

Received 2 June; accepted 28 June 2005.

1. Wilson, P. A. & Norris, R. D. Warm tropical ocean surface and global anoxia during the mid-Cretaceous period. *Nature* **412,** 425–429 (2001).
2. Norris, R. D., Bice, K. L., Magno, E. A. & Wilson, P. A. Jiggling the tropical thermostat in the Cretaceous hothouse. *Geology* **30,** 299–302 (2002).
3. Dean, W. E., Arthur, M. A. & Stow, D. A. V. Origin and geochemistry of Cretaceous black shales and multicoloured claystones, with emphasis on Deep Sea Drilling Project Site 530, southern Angola Basin. *DSDP Init. Rep.* **75,** 819–844 (1984).
4. Erlich, R. N., Palmer-Koleman, S. E. & Antonieta Lorente, M. Geochemical characterization of oceanographic and climatic changes recorded in upper Albian to lower Maastrichtian strata, western Venezuela. *Cretac. Res.* **20,** 547–581 (1999).
5. Rusk, D. C. in *Petroleum Provinces of the Twenty-first Century* (eds Downey, M. W., Threet, J. C. & Morgan, W. A.) 429–452 (Memoir 74, AAPG, Tulsa, 2001).
6. Hofmann, P., Wagner, T. & Beckmann, B. Millennial- to centennial-scale record of African climate variability and organic carbon accumulation in the Coniacian-Santonian eastern tropical Atlantic (Ocean Drilling Program Site 959, off Ivory Coast and Ghana). *Geology* **31,** 135–138 (2003).
7. Beckmann, B., Wagner, T. & Hofmann, P. in *The Deposition of Organic-Carbon-Rich Sediments: Models, Mechanisms, and Consequences* (ed. Harris, N. B.) 125–143 (Spec. Publ. 82, SEPM, Washington, 2005).
8. Wagner, T., Sinninghe Damsté, J. S., Hofmann, P. & Beckmann, B. Euxinia and primary production in Late Cretaceous eastern equatorial Atlantic surface waters fostered orbitally driven formation of marine black shales. *Paleoceanography* **19,** doi:10.1029/2003PA000898 (2004).
9. Calvert, S. E. in *Treatise on Chemical Oceanography 6* (eds Riley, J. P. & Chester, R.) 187–280 (Academic, San Diego, 1976).
10. Zabel, M. *et al.* Late Quaternary climate changes in Central Africa as inferred from terrigenous input to the Niger Fan. *Quat. Res.* **56,** 207–217 (2001).
11. Diester-Haass, L. & Chamley, R. C. Palaeoceanographic and palaeoclimatic evolution in the Wedell Sea (Antarctica) during the middle Eocene-late Oligocene, from a coarse sediment fraction and clay mineral data (OCP 689). *Mar. Geol.* **114,** 233–250 (1993).
12. Yarincik, K. M., Murray, R. W. & Peterson, L. C. Climatically sensitive eolian and hemipelagic deposition in the Cariaco Basin, Venezuela, over the past 578,000 years: Results from Al/Ti and K/Al. *Paleoceanography* **15,** 210–228 (2000).
13. DeConto, R. M., Hay, W. W., Thompson, S. L. & Bergengren, J. in *The Evolution of the Cretaceous Ocean-Climate System* (eds Barrera, E. & Johnson, C.) 391–406 (Spec. Pap. 332, Geol. Soc. Am., Boulder, 1999).
14. Holbourn, A. E. L. *et al.* in *The Oil and Gas Habitats of the South Atlantic* (eds Cameron, N. R., Bate, R. H. & Clure, V. S.) 195–222 (Spec. Publ. 153, Geol. Soc., London, 1999).
15. Wagner, T. Late Cretaceous to early Quaternary organic sedimentation in the eastern equatorial Atlantic. *Palaeogeogr. Palaeoclimatol. Palaeoecol.* **179,** 113–147 (2002).
16. Rey, O., Simo, J. A. & Lorente, M. A. A record of long- and short-term environmental and climatic change during OAE3: La Luna Formation, Late Cretaceous (Santonian-early Campanian), Venezuela. *Sedim, Geol.* **170,** 85–105 (2004).
17. Thompson, S. L. & Pollard, D. A global climate model (GENESIS) with a land-surface-transfer scheme (LSX). Part 1: Present-day climate. *J. Clim.* **8,** 732–761 (1995).
18. Bice, K. L., Barron, E. J. & Peterson, W. H. Continental runoff and early Cenozoic bottom-water sources. *Geology* **25,** 951–954 (1997).
19. Alychunskaya, N. M. & Ivanov, V. V. in *World Water Balance and Water Resources of the Earth* (ed. Korzun, V. I.) 568–574 (Studies and Reports in Hydrology 25, UNESCO, Paris, 1978).
20. Hay, W. W., *et al.* in *The Evolution of the Cretaceous Ocean-climate System* (eds Barrera, E. & Johnson, C.) 1–48 (Spec. Pap. 332, Geol. Soc. Am., Boulder, 1999).
21. Watkins, D. K., Shafik, S. & Shin, I. C. Calcareous nannofossils from the Cretaceous of the Deep Ivorian Basin. *ODP Sci. Res.* **159,** 319–333 (1998).
22. Kuhnt, W., Moullade, M. & Kaminski, M. A. Upper Cretaceous, K/T boundary, and Paleocene agglutinated foraminifers from Hole 959D (Côte d'Ivoire-Ghana Transform Margin). *ODP Sci. Res.* **159,** 389–411 (2004).
23. Shipboard Scientific Party. Explanatory notes. *Proc. ODP Init. Rep.* **207,** 1–94 (2004).

Supplementary Information is linked to the online version of the paper at www.nature.com/nature.

Acknowledgements We thank the Ocean Drilling Program for providing the sample material and technical assistance. H. Heilmann, R. Henning, B. Kockisch, M. Gölden, S. Berg, A. Katzemich, S. Reiss, M. Aiyswaryan, R. Kunze and D. Pollard are thanked for analytical assistance.

Author Information Reprints and permissions information is available at npg.nature.com/reprintsandpermissions. The authors declare no competing financial interests. Correspondence and requests for materials should be addressed to T.W. (thomas.wagner@ncl.ac.uk).